J Fluoresc (2013) 23:813–821
DOI 10.1007/s10895-013-1181-2

ORIGINAL PAPER

Comprehensive Study on the Binding of Iron Schiff Base Complex with DNA and Determining the Binding Mode

Maryam Nejat Dehkordi · Per Lincoln

Received: 28 September 2012 / Accepted: 24 February 2013 / Published online: 22 March 2013

Abstract The iron (III) [N, N′ Bis (5-(triphenyl phosphonium methyl) salicylidene)-1, 2 ethanediamine] chloride [Fe Salen] Cl, has been synthesized and characterized as described previously. The interaction of iron complex with calf thymus (CT) DNA has been studied extensively by experimental techniques. Absorption spectra showed both hypochromism and hyperchromism. Thermal denaturation study of DNA with complex revealed the ΔT_m of 5 °C. Competitive binding study shows that the enhanced emission intensity of ethidium bromide (EB) in the presence of DNA was quenched by adding of the iron complex indicating that it displaces EB from its binding site in DNA and the apparent binding constant has been estimated to be $5\times10^6\,\mu M^{-1}$. Fluorescence Scatchard plot revealed type B behavior for interaction of complex to DNA. Circular dichroism (CD) spectra measurements showed that the complex interacts with DNA via surface and groove bindings. Linear dichroism (LD) measurements confirmed the bending of DNA in the presence of complex. Furthermore, Isothermal titration calorimetry (ITC) experiments approved that the binding of complex is based on both electrostatic and hydrophobic interactions. More, ITC profile exhibits the existence of two binding phases for the complex.

Keywords Schiff base · ct-DNA · Fluorescence · Circular dichroism (CD) · Linear dichroism (LD) · Isothermal titration calorimetry (ITC)

M. Nejat Dehkordi (✉)
Department of Chemistry, Faculty of Science,
Islamic Azad University, Shahrekord branch,
Shahrekord, Iran
e-mail: nejatmary@yahoo.com

M. Nejat Dehkordi
e-mail: mnejatdehkordi@gmail.com

P. Lincoln
Department of Chemical and Biological Engineering, Chalmers
University of Technology, 412 96 Gothenburg, Sweden

Introduction

Among the organic compounds, Schiff bases possess excellent properties such as, structural similarities with natural biological substances, simple preparation procedures, flexibility in synthesis, wide applications, and diverse structure modification [1, 2].

Schiff bases have been reported to show a variety of biological actions by virtue of the azomethine linkage, which is responsible for various antibacterial, antifungal, herbicidal, clinical and analytical activities [3–6].

Schiff base complexes have been widely studied due to the numerous applications. They serve as models for biologically important species and find applications in biomimetic catalytic reactions. Chelating ligands containing N, S and O donor atoms show broad biological activity and they are of special interest due to the variety of ways in which they are bonded to metal ions. It is known that the existence of metal ions bonded to biologically active compounds may enhance their activities [7–12].

Schiff bases have potential for anticancer drugs. The anticancer activity of this compound will increase when they complex with metal ions [13, 14].

There has been useful progress in designing and synthesis of new anticancer agents. To obtain more selective agents, exhaustive knowledge of DNA-binding mechanisms is required [15]. Meanwhile, Metal Salen complexes display significant interaction with DNA and all the investigated transition metal Salen complexes showed the ability to cleave DNA via redox process [16–21]. In previous research, the interaction of a number of iron derivatives and iron ions with the anticancer antibiotic adriamycin and nucleic acids has been widely investigated [22–24]. Moreover, it has been proved that Fe (III)-Salen derivatives have the potential for DNA damage and biochemical activity and also they have effects on viability of cultured human cells [25].

In some cases, they have shown AT-selective binding and photonuclease activity as a minor groove [26].

Iron Schiff base complexes have been used as netropsin models to describe the redox active metal ions in DNA binding process also, iron Schiff base complexes exhibit a catalytic activity toward the bland oxidation of hydrocarbons analogously to other porphyrin complexes [27]. These compounds undergo electron transfer reactions, mimicking the catalytic functions of peroxidases [28]. In order to develop the chemistry of Iron Schiff base complexes specifically in biomedical application [29–31], we have focused on the interaction of bulky Salen-type complex of iron with DNA. The iron (III) [N, N′ Bis (5-(triphenyl phosphonium methyl) salicylidene)-1, 2 ethanediamine] chloride is five coordinate (square pyramidal) with axial chloride (Fig. 1). The axial ligand could be replaced with solvent molecules and in solution; complex is a square planar in the middle. This complex contains two bulky groups on the phenyl rings of ligand that influence the overall properties of complex specifically in the catalytic properties. As stated before, increasing the steric hindrance about the metal center of complex affects its reactivity and these effects are not straightforward. In some cases, sterically hindered complexes have been shown to react faster in catalytic reactions in comparison to less bulky ones [32]. In one side, this complex contains two positive charges that make it soluble in water and on the other hand, the complex contains bulky aryl groups that make it hydrophobic. Therefore, it seems that the complex is proper for interaction with DNA due to both hydrophobic and hydrophilic parts. Additionally, it was interesting to us to investigate the effect of sterically hindered bulky groups of the iron Salen complex on the DNA binding process. We predicted that these groups will increase the interaction of complex with DNA despite the loss of significant flat part on the complex. We wanted to show that the bulky groups in the iron Salen complex increase the DNA binding process too, likewise the increase on the catalytic activity [32]. Therefore, to achieve this aim, the interaction of the iron complex with native DNA was investigated with valuable and exhaustive techniques such as UV–vis, Fluorescence, Circular and Linear dichroism and ITC. So, the experimental data were analyzed and interpreted for determining the binding mode.

Experimental

Materials and Methods

The substituted phosphonium bulky Salen type ligand and its iron complex were synthesized with using standard procedure of refluxing ethanolic solutions of corresponding ethylendiamine and substituted salicylaldehyde in a 1:2 mol ratio for ligand. The complex was synthesized with using $FeCl_3$ as described previously in four steps [32, 33]. Synthesis and characterization of ligand and complex have been reported in the literature; therefore, its purity was only checked by ^{1}H NMR and infrared spectroscopy as follow:

> Ligand (yellow powder): Significant IR bands (KBr, υ cm^{-1}): υ_{OH} 3420 (broad), $\upsilon_{C=N}$ 1630, UV–vis λ_{max} (nm) in H2O: 405, 225, $\delta_{\mathbf{H}}$ (D_2O): 4 (4 H, s, CH_2N), 4.54 (4 H, d, CH_2P), 6.5 (2 H, d, Ar), 7.1 (2 H, d, Ar), 7.4 (2H, m, Ar) 7.56–7.69 (30 H, m, Ph), 8.06 (2 H, s, CH = N).

Iron Salen complex (Dark red powder): Significant IR bands (KBr, υ cm^{-1}): υ_{H2O} 3385 (broad), $\upsilon_{C=N}$ 1615. Since the iron (III) is paramagnetic in nature, its NMR spectrum could not be obtained.

Double stranded calf thymus DNA (sodium salt, highly polymerized type I) was purchased from Sigma and dissolved in buffer and filtered with a 0.8 μM Millipore filter before using. The DNA concentration was determined using ε_{260nm}=6,600 $M^{-1}cm^{-1}$. The ratio of A_{260}/A_{280} for solution of ct-DNA in buffer was 1.8–1.9 that represents the free protein DNA sample [34, 35]. Other regents were purchased commercially and used without further purification. All experiments were carried out in a 10 mM Tris–HCl aqueous buffer at pH=7.2 and 5 mM NaCl.

DNA Binding Studies

Instrumentation

The electronic absorption spectra were recorded on a Varian Cary 4000 UV–vis spectrophotometer operating with the parameters: 200 to 800 nm, 1 cm path-length cuvettes, double beam mode, bandwidth 1 nm. The absorbance titrations were performed at a fixed concentration of iron Salen

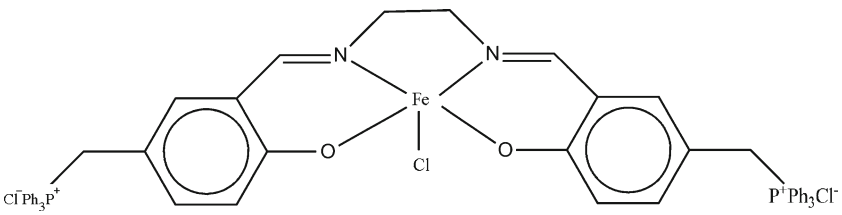

Fig. 1 Iron (III) [N, N′ Bis (5-(triphenyl phosphonium methyl) salicylidene)-1, 2 ethanediamine] chloride

(8 and 21 μM) while varying the DNA concentration of (0–150 μM and 0–94 μM) base pairs. In order to eliminate the absorbance of DNA, an equal amount of DNA was added to both sample solution and reference cuvette and absorbances were recorded after each successive addition of DNA.

Melting experiments were performed using Carry-4000 spectrophotometer in conjunction with a thermostated cell compartment. These measurements were carried out in 10 mM Tris/HCl buffer, pH =7.2 containing 50 μM DNA and 10 μM of iron complex. The temperature inside the cuvette was determined with a platinum probe and was increased over the range of 20–90 °C at a heating rate of 1 °C/min (Thermal software). The melting temperature, Tm, was obtained from the mid-point of the hyperchromic transition.

Fluorescence measurements were performed on a Varian Cary Eclipse spectrofluorimeter. Emision spectra were recorded at an excitation wavelength of 515 nm and the emission spectra were recorded from 525 nm to 800 nm. Both excitation and emission slits were set as 5 nm. In competition binding experiments, DNA and Ethidium Bromide (EB) concentrations were 45 μM and 4.9 μM, respectively, while complexes varied from 0 to 26.5 μM. In the reverse titrations DNA samples (40 μM) with different concentration of complex (0.79, 2, 4 and 8 μM) were titrated with EB (from 1 to 19 μM). The excited wavelength was 515 nm and the emission observed at 605 nm.

Circular dichroism (CD) was recorded with a Chirascan CD spectrometer (Applied Photophysics, UK). The wavelength interval was 200–600 nm, bandwidth 1 nm with steps of 1.0 nm. The time-per-point was 0.5 s. The spectra were recorded in a 1 cm cell and each spectrum is the average of four scans from 200 to 600 nm. The spectrum recorded immediately without incubating. DNA concentration in this experiment is 45 μM that titrated with complex from 3.8 to 68 μM.

Linear dichroism (LD) was measured using a spectrometer (Applied Photophysics, UK). The wavelength interval was 200–600 nm. For LD measurements, DNA solution was 100 μM and iron complex from 7.5 to 91 μM. The spectrum was measured in a cylindrical flow cell containing 2 mL of DNA solution. The DNA was oriented by a flow gradient of 1,000 rpm in a Couvette cell with an outer rotating cylinder ensuring no bubbles were present in the cell.

Isothermal titration calorimetry (ITC) measurements were carried out at 25.0 °C using a Microcal (Microcal, Inc., Northampton, MA). The sample cell was loaded with 300 μL of 100 μM of DNA solution and Titration was carried out using a 40 μL syringe filled with 1,400 μM of the iron complex solution, with stirring at 1,000 rpm. A titration experiment consisted of 20 consecutive injections of 2 μL volume, 4 s duration of each injection, with a 3 min interval between injections. The initial delay before the first injection was 60 s. To correct the heat effects of dilution and mixing, a control experiment was performed by injecting the complex into the buffer solution. Calorimetric data for DNA binding of the complex were analyzed using MicroCal Origin software version 7 supplied with the instrument. The dilution heat of injecting the DNA into the buffer was observed to be negligible. All the solutions were degassed before using. Each of the heat burst curve in the figure correspond to a single complex injection. The areas under these heat burst curves were determined by integration to yield the associated injection heats. These injection heats were corrected by subtracting the corresponding dilution heats derived from the injection of identical amounts of complex into buffer alone. The resulting corrected injection heats are plotted against complex to DNA molar ratios.

Result and Discussion

Studies with DNA

UV–vis Absorption Spectroscopy and DNA Binding Interaction

Iron complex exhibits an intense absorption bands at UV region about 225 nm and shoulders at 260, 300, 400 nm. By adding DNA to a fixed concentration of complex slightly hyperchromism was observed above 300 nm and also a hypochromism (14 %) was seen below the 300 nm without any red shift (see Fig. 2). The observed hypo and hyperchromism on the spectra by adding the DNA to complex, is indicative of both electrostatic and hydrophobic interactions. As stated before, this complex has a replaceable

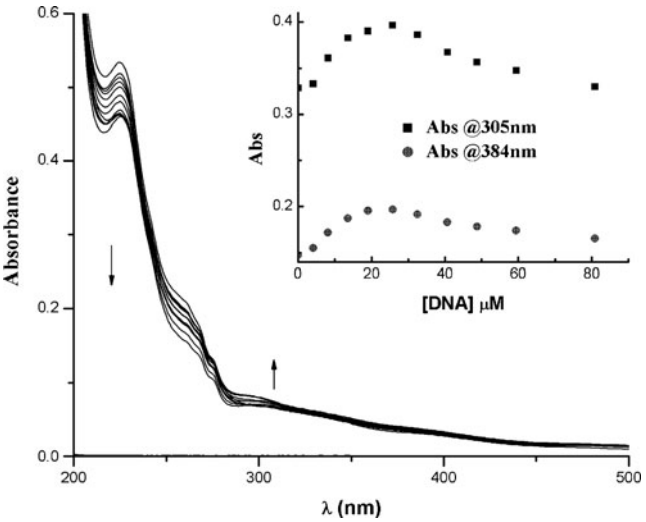

Fig. 2 Absorption titration spectra of Fe Salen complex (8 μM) in the presence of increasing amounts of ct-DNA (0–150 μM) in 10 mM Tris–HCl/5 mM NaCl, pH=7.2, *Arrow* shows the absorbance changes upon increasing DNA concentration. The *inset plot* shows the changes on the absorbance of the Fe Salen complex (21 μM) in the presence of DNA against the DNA concentration above 300 nm

chloride ligand in solution, which may be replaced with H_2O molecules [36]. Therefore, in solution, the complex has a flat part or square planar with a positive charge in the middle and two positive charges on the both sides of complex. In this regard, the positively charged complex can interact with phosphate back bone and also coordination of Fe^{3+} with donor atoms on the base pairs of the DNA is possible. The hyperchromism on the spectra is the result of the electrostatic interaction between the complex and DNA [37, 38]. Then the surface binding interactions keep the complex next to the DNAs and the phenyl rings on the phosphonium groups may be entangled between the grooves of DNA and cause the hydrophobic interactions [39, 40]. Therefore, the hydrophobic interactions lead to the hypochromic effect on the spectra [41–43].

The inset of figure is absorption data of the iron complex in the presence of different DNA concentrations. This figure shows both increase and decrease in the absorption of Fe Salen complex above the 300 nm. This plot demonstrates that two different binding modes might be involved in the progress of interaction thereby the hypo and hyperchromism are seen in the spectra.

Thermal Denaturation Study

To determine the conformational changes and the strength of DNA binding affinity toward small molecules thermal denaturation study was done. It is known that double stranded DNA gradually dissociates to single strands with increasing solution temperature and results in a hypochromic affect [44]. T_m is strictly related to the stability of double helix, and the interaction of the molecules with DNA may alter the T_m by stabilizing or destabilizing the final complex.

The stabilization of the DNA double helix from the stabilizing stacking interactions is followed by a considerable increase in the melting temperature of DNA [45, 46]. While the primary groove and/or electrostatic binding of the complexes to DNA stabilize the DNA double helix structure and will cause low increase in ΔT_m. The melting curves of DNA solution in the absence and presence of complex were obtained by plotting the absorbance at 260 nm as a function of temperature (see Fig. 3). The increase in thermal stability of DNA due to addition of iron complex is about 5 °C. This result shows that the complex interacts with DNA via non-intercalation binding. By considering the structure of the complex and the observed increase in T_m, the surface and groove binding are the possible interaction between the complex and DNA.

Fluorescence Study

To investigate the binding of iron complex to DNA by intercalation, an emission quenching experiment has been carried out and Ethidium Bromide was employed. It is known that

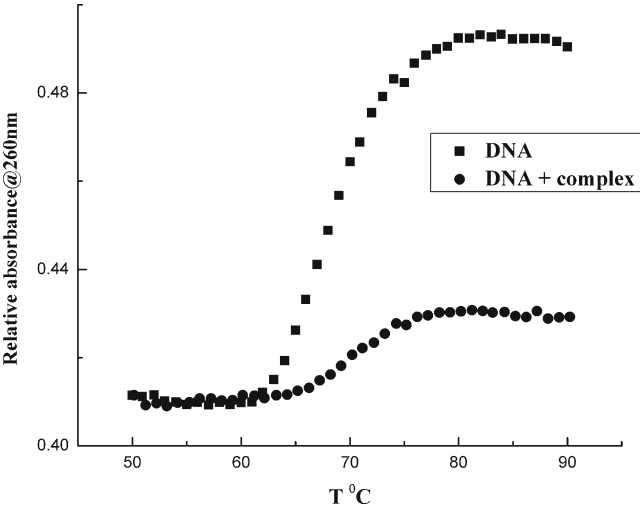

Fig. 3 Melting curve of ct-DNA (50 μM) at 260 nm in the absence (*black square*) and presence (*black circle*) of Fe Salen complex (10 μM)

DNA solution is not fluorescence and EB is also weakly fluorescence but the EB-DNA is fluorescence due to the intercalation of EB between adjacent DNA base pairs [47]. The intense decrease of EB-DNA emission due to the addition of iron complex was observed (see the inset of Fig. 4). This phenomenon could be from the competition of the complexes with EB for the same binding sites on DNA resulting release of EB from DNA. To determine quantitatively the affinity of the iron complex to DNA, the binding constant for the iron complex was calculated. In this regard, the experimental data of free and bound EB (Fig. 5), in each titration were fitted to

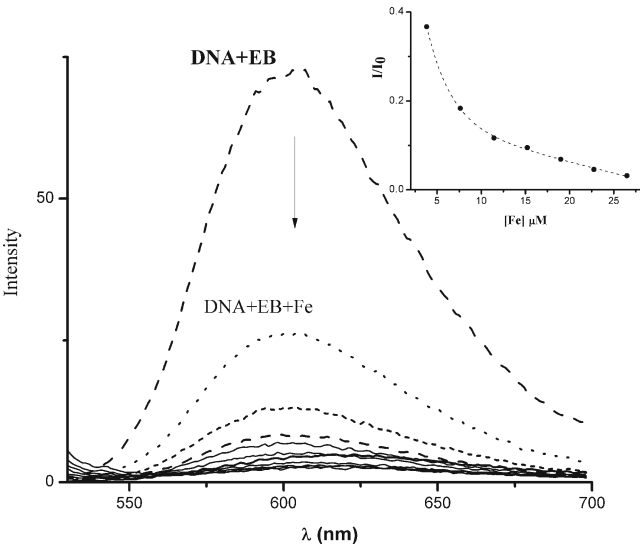

Fig. 4 The emission spectra of DNA-EB (45 and 4.9 μM), λ_{ex}= 515 nm, $\lambda_{max\text{-}em}$=605 nm, in the presence of 0–26.5 μM Fe Salen complex. *Arrow* shows the intensity changes upon increasing the Fe Salen complex. *Inset*: the plot of the relative fluorescence intensity at 605 nm vs total concentration of Fe Salen complex

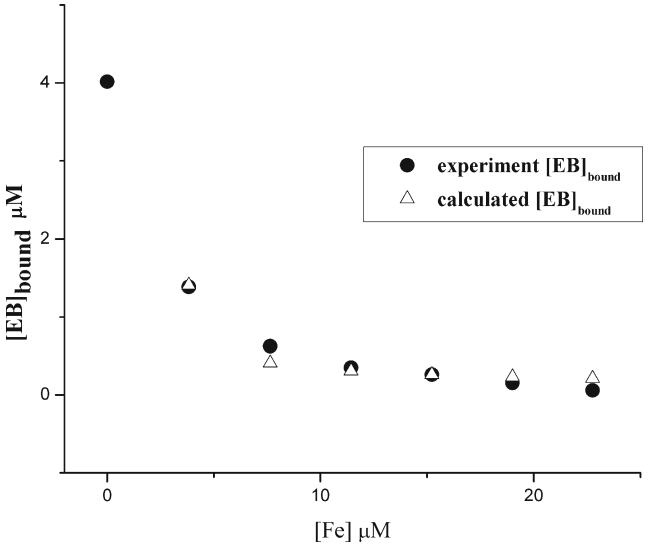

Fig. 5 The comparison of experimental and calculated data of bound EB that fitted with McGhee-Von Hipple equation by the MATLAB program, vs total concentration of Fe Salen complex

McGhee and Von Hipple conditional probability model of excluded site binding according to Eq. (1) [48, 49].

$$\theta_{EB}/C_f = K_{EB}(1 - s\theta_{EB})[(1 - s\theta_{EB})/(1 - (s-1)\theta_{EB})]^{s-1} \quad (1)$$

Where K_{EB} is the apparent binding constant of EB and s is the apparent binding site size. The θ_{EB} is the ratio of bound EB to the number of DNA base pairs. The values 0.5×10^6 μM and 2 were considered for binding constant and the size of binding site of EB as reported in the literature.

The value of $5\times10^6\,\mu M^{-1}$ was obtained for the iron Salen complex that shows the strong affinity of complex to DNA in comparison to other Salen complexes reported on the literature. Even the interaction of this complex is considerable related to the iron Salen complex without any substituted group on the phenyl rings.

Determining of the Binding Mode of Iron to DNA by Fluorescence Measurments

According to the fluorescence experiment, it is clear that the complex competes with EB for the binding sites, but what kind of binding between the complex and DNA will occur? To respond to this question, we have used the Scatchard approach to distinct between the intercalation and other interactions.

In order to understand how the EB–DNA binding is affected by the iron complex, Fluorescence Scatchard plots of the binding of EB to ct-DNA in the absence and the presence of various amount of iron complex were determined. Each sample containing DNA and iron complex was titrated with EB stock solution. All measurements were carried out at room temperature. Binding isotherms in the presence of the iron complex depicted in Fig. 6 and the corresponding Scatchard plots constructed. A set of straight lines were obtained. They show that complex belongs to class B. The B class is a set of compound that non-competitively inhibits the binding of EB to DNA. Thus, the iron complex binds covalently to the DNA at sites other than those occupied by EB and prevents the binding of EB. In spite of the covalent bond other type of interaction with DNA are probable. It means that the complex may bound covalently or bound in grooves of DNA and inhibit insertion of EB to the binding sites on DNA [50, 51].

Circular Dichroism Studies

The iron complex was not optically active and therefore did not exhibit any CD spectra, but ct-DNA in the B form conformation shows two conservative CD bands in UV region: a positive band at 278 nm due to base stacking and a negative band at 246 nm due to right handed helicity of DNA.

Since different DNA structures (A, B, Z, and C) have different spectroscopic shapes in CD, This technique is a powerful way to understand the conformational changes of B-DNA. Classical intercalation reactions tend to enhance the intensities of bands due to the strong base stacking interactions and stable DNA conformations, while simple groove binding and electrostatic interactions with small molecules show less perturbation or no perturbation on the base stacking and helicity bands [52].

CD spectrum of DNA in the presence of iron complex exhibits an increase in both positive and negative peaks with a blue shift in the positive band positions at 0.49 mol ratio of

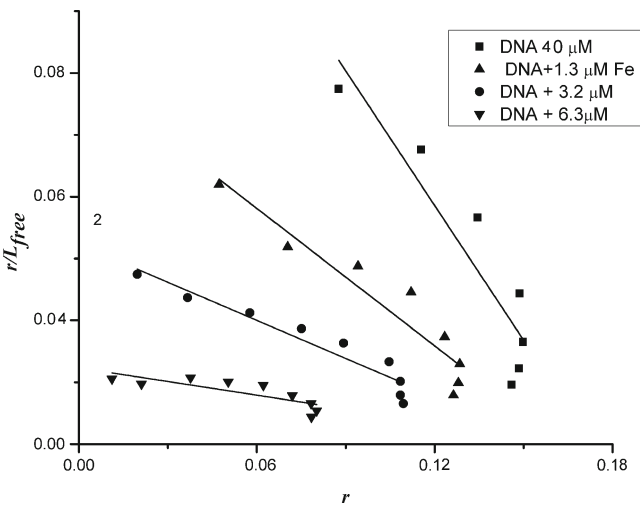

Fig. 6 Fluorescence Scatchard plots for the binding of EB to DNA in the absence and presence of various amounts of Fe Salen complex. [DNA]=40 μM and EB concentration varied from 1 to 19 μM

Iron Salen complex to DNA. There was a weak indication of induced CD above 300 nm (see Fig. 7).

A large fluctuation in the CD spectra was observed in high concentration of complex in mole ratio more than 0.49. Therefore, it seems that in high concentration; the complex induces the formation of supramolecular DNA aggregation.

As we know the complex is bulky with a flat part in the middle therefore, the increase in the CD bands could not be due to the intercalation of complex between the base pairs. Then, to interpret this increase, it could be stated that the complex interacts with DNA by electrostatic interaction at the beginning or by forming bridge between the duplexes. Namely, the electrostatic interactions keep the complex next to the DNAs and then the phenyl rings on both sides of the complex could interact with two neighboring DNAs and form the adducts. Since, the formed adducts are stabilized by hydrophobic interactions or columbic interactions as shown in the case of Cu $(bcp)_2^+$ [53], therefore the increase in the positive CD band is seen.

Besides, the neutralization of the surface charges of DNA could happen due to the strong electrostatic interactions between the iron complex and DNA and as a result the helicity of DNA increases and more bent of DNA occurs. In such a way, the increase in the negative band is observed too.

Furthermore, the positive charges of the complex and electrostatic attraction to the anionic phosphate backbone of DNA cause more wounding of DNA and the interaction of bulky phenyl rings moiety with grooves of DNA cause releasing of water from the grooves and the DNA transforms from B to A structure. The blue shift on the spectrum is the result of this transform.

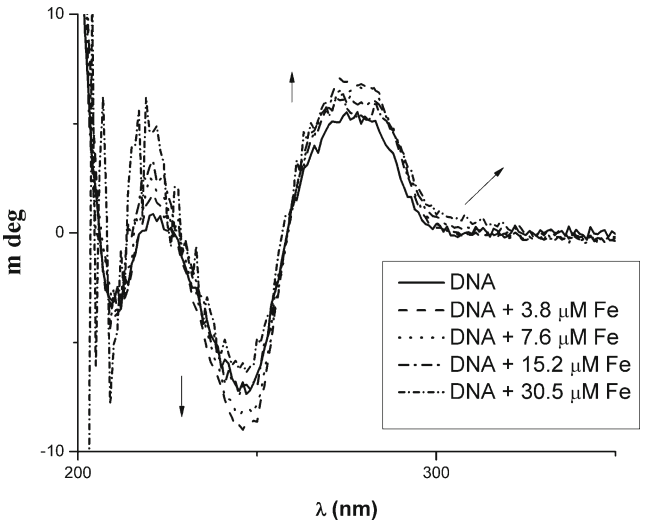

Fig. 7 CD spectra of ct-DNA in the absence and presence of Fe Salen complex. *Arrows* show the CD changes upon increasing the Fe Salen concentration

Finally, the CD spectra and geometry of DNA are significantly perturbed in mole ratio 0.5 that it may be indicative of aggregation of DNA with iron complex.

Isothermal Titration Calorimetry Studies

Isothermal titration calorimetry has become an important tool in direct and reliable measuring of the thermodynamic parameters of the interaction of small molecules with biopolymers [54].

The representative raw ITC profile results from the titration of iron complex into DNA solution. Each of the heat burst curves corresponds to a single iron complex injection. The areas under these heat burst curves were determined by integration to yield the associated injection heats. These injection heats were corrected by subtracting the corresponding dilution heats derived from the injection of identical amounts of iron into the buffer alone. ITC profile for the binding of the iron complex to DNA is shown in Fig. 8. First, the titration curve displayed that the binding of the complex to DNA was endothermic with positive peaks, and then exothermic with negative peaks in the plots of power versus time. The first binding is overwhelmingly entropy driven, while the second binding is enthalpy driven. It seems that, in the first step entropy term arises from liberation of structured water from interacting surfaces and releasing of counter ions upon binding of positively charged complex to the backbone of DNA helix [55, 56]. These results are correspond to the CD results too.

On the other hand, in the second step, the process must be enthalpy driven with a decrease in enthalpy due to the effect of more hydrophobic interactions.

It is worthy to note that the two phases of the binding had been seen by the absorption data too.

Linear Dichroism Measurements

Linear dichroism (LD) is defined as the difference in absorbance between light polarized parallel ($A_\parallel$) and perpendicular ($A_\perp$) to a macroscopic orientation axis.

$$LD(\lambda) = A_\parallel(\lambda) - A_\perp(\lambda)$$

To detect an LD signal, a sample with oriented molecules is needed. Large molecules like DNA can be oriented by a flow gradient (flow-LD in a couette cell). DNA in the B form shows the negative LD-signal at 260 nm, due to the base π–π^* transitions. These transition moments will be aligned perpendicular to the orientation axis. The magnitude of this LD signal depends on the degree to which DNA is oriented and reduced by effects such as DNA binding.

When a small molecule bound to DNA in a specific way, it will be aligned with the DNA and the binding of the

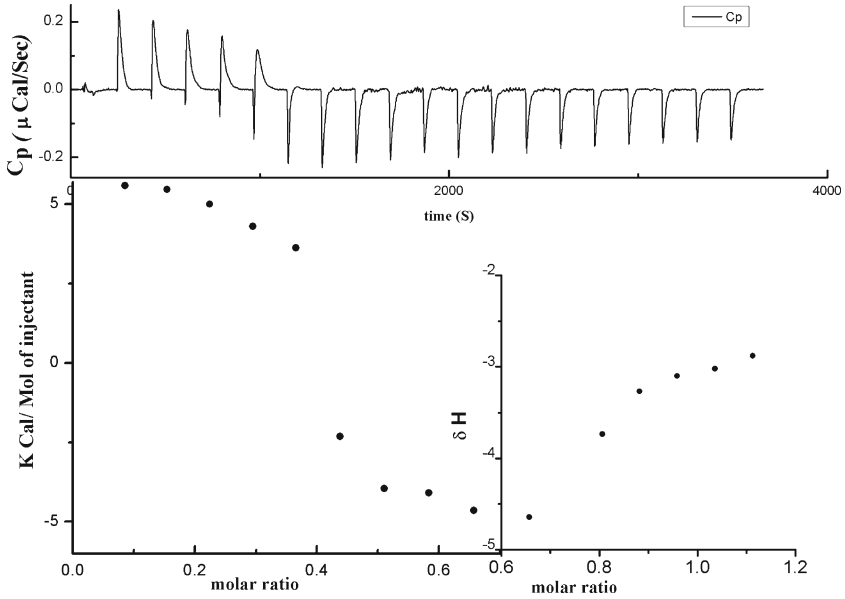

Fig. 8 Calorimetric data (*raw*) for the titration of DNA 100 μM with iron complex at 25 °C (*top*). Binding isotherm (heat changes vs [Fe-complex]/[DNA] molar ratio) was obtained from the integration of raw data (*bottom*)

ligand can be investigated by the changes in the LD signal of DNA. Planar molecules intercalated into DNA will have the transition moments parallel to the plane of bases and show a negative LD signal. On the other hand, if a molecule binds in the grooves of DNA, its transition moments, will be more parallel to the DNA helix and show a positive LD-signal.

Since, this technique has shown to be an efficient tool to evaluate the binding mode between DNA and complexes [57, 58]; thus, the LD spectra of Iron complex in the presence of DNA were measured as shown in Fig. 9. The LD signal of DNA in the presence of different concentration of iron complex decreases and it disappears in mole ratio more than 0.6. The LD signal of DNA arising the bases is significantly reduced by the addition of concentration of complex.

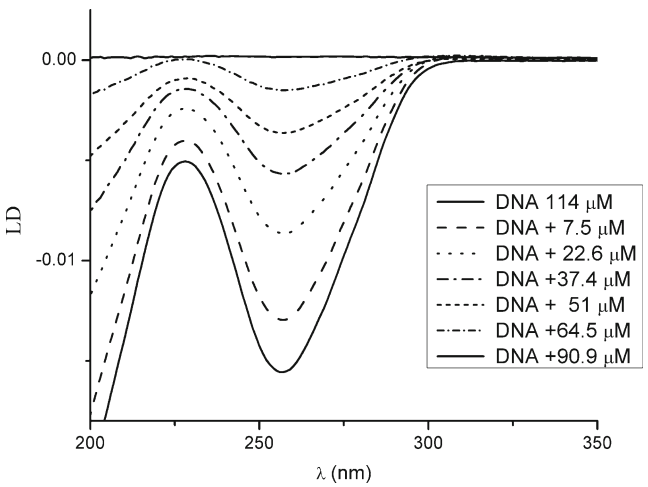

Fig. 9 LD spectra of ct-DNA in the absence and presence of Fe Salen complex

This could be resulted from either an increase in DNA flexibility or shortening of the DNA by bending, kinking, compaction or aggregation. Such a behavior was observed for the LD measurements of platinium complexes with DNA before [59].

More, the other reason for decreasing the LD signal of DNA is coordination of Fe^{+3} with donor atom on the base pairs of DNA as explained in the absorbance experiment.

Also, wounding or aggregation of DNA occurs in the presence of complex at high concentration.

Conclusions

This work reports the binding properties of iron complex with DNA. The binding constant of iron complex has been determined by the fluorescence data that indicates strong binding affinity of the complex to DNA. It has been found that the iron complex stabilizes the ct-DNA thermally up to 5 °C that demonstrates non-intercalative binding with DNA. Besides, the increase in the positive CD band of DNA could be indicative of the interaction of phenyl rings with the grooves and formation of adducts due to the electrostatic and hydrophobic effects. The decrease on the LD signal of DNA shows that the complex can bend or aggregate the DNA. More, this claim is confirmed by increasing on the negative CD band of DNA. A competitive binding study showed that the enhanced emission intensity of EB in the presence of DNA was quenched by adding the iron complex. Thus, the iron complex displaces EB from its binding site in DNA. Fluorescence Scatchard plot exhibits the type B behavior for binding mode.

The ITC result confirms two binding phases for the complex. The binding process is endothermic in the first

step (entropy driven) and exothermic in the second step (enthalpy driven).

Therefore, the set of results demonstrated that bulky iron Salen complex interacts with DNA via electrostatic interaction at the beginning and the surface interaction between the complex and DNA lead to the coordination of Fe^{3+} with the donor atom on the base pairs of DNA. This interpretation was approved by the UV–vis data and fluorescence Scatchard plots.

Finally, it should be emphasized that this Salen complex strongly binds to DNA compared to iron Salen complex without substituent on the phenyl rings as reported by Silvestri et al. Also, interaction of this complex is considerable against other Salen complexes with less bulky groups such as NH_3^+ as reported in the literatures. The bulky and hydrophobic groups on the ligand have increased the interaction of complex with DNA and the effect of these groups is straightforward in binding process too. Hence, regarding to the results of DNA binding of iron complex, it seems that this complex is valuable for more research such as biological activity toward the cells. In future work, we decide to investigate the in vitro DNA cleavage properties and its biochemical effects on the cultured human cells.

Acknowledgments The financial support of Research Councils of Islamic Azad University of Shahrekord and Chalmers University are gratefully acknowledged. Also we are thankful of Professor Valliolah Mirkhani for his useful guides.

References

1. Coles SJ, Hursthouse MB, Kelly DG, Toner AJ, Walker NM (1998) Halide titanium(IV) Schiff base complexes; fluoride and bromide derivatives and evidence for a new seven-coordinate chloride intermediate. J Chem Soc Dalton Trans 3489
2. Jungreis E, Thabet S (1969) Analytical applications of Schiff bases. Marcell Dekker, New York
3. Jarrahpour AA, Motamedifar M, Pakshir K, Hadi N, Zarei M (2004) Synthesis of novel Azo Schiff bases and their antibacterial and antifungal activities. Molecules 9:815–824
4. Mohindru A, Fisher JM, Rabinovitz M (1983) Bathocuproine sulphonate: a tissue culture-compatible indicator of copper-mediated toxicity. Nature (London) 64:303
5. Palet PR, Thaker BT, Zele S (1999) Preparation and characterisation of some lanthanide complexes involving a heterocyclic β-diketone. Indian J Chem 38(6)A:563
6. Yang TL, Tai XS, Qin WW, Liu WS, Tan MY (2004) Determination of trace terbium(III) with N, N′, N″-Tri(3-indolemethanal)triaminotriethylamine based on a new fluorescence enhancement system. Anal Sci 20:357–361
7. Singh K, Barwa MS, Tyagi P (2007) Synthesis and characterization of cobalt(II), nickel(II), copper(II) and zinc(II) complexes with Schiff base derived from 4-amino-3-mercapto-6-methyl-5-oxo-1,2,4-triazine. Eur J Med Chem 42:394–402
8. Cozzi PG (2004) Metal–Salen Schiff base complexes in catalysis: practical aspects. Chem Soc Rev 33:410–421
9. Chandra S, Sangeetika J (2004) EPR and electronic spectral studies on copper(III) complexes of some NO donor ligands. J Indian Chem Soc 81:203–206
10. Ferrari MB, Capacchi S, Pelosi G, Reffo G, Tarasconi P, Albertini R, Pinelli S, Lunghi P (1999) Synthesis, structural characterization and biological activity of helicin thiosemicarbazone monohydrate and a copper(II) complex of salicylaldehyde thiosemicarbazone. Inorg Chim Acta 286:134–141
11. Canpolat E, Kaya M (2004) Studies on mononuclear chelates derived from substituted Schiff-base ligands (part 2): synthesis and characterization of a new 5-bromosalicyliden-p-aminoacetophenone oxime and its complexes with Co(II), Ni(II), Cu(II) and Zn(II). J Coord Chem 57:1217–1223
12. Yildiz M, Dulger B, Koyuncu SY, Yapici BM (2004) Synthesis and antimicrobial activity of bis(imido) Schiff bases derived from thiosemicarbazide with some 2-hydroxyaldehydes and metal complexes. J Indian Chem Soc 81:7–12
13. Gungora E, Celenb S, Azazb D, Karaa H (2012) Two tridentate Schiff base ligands and their mononuclear cobalt (III) complexes: Synthesis, characterization, antibacterial and antifungal activities Spectrochim. Acta Part A 94:216–221
14. Liu Y-C, Yang Z-Y (2010) Antioxidation and DNA-binding properties of binuclear Er(III) complexes with Schiff-base ligands derived from 8-hydroxyquinoline-2-carboxaldehyde and four aroylhydrazines. J Biochem 147(3):381–391
15. Alonso A, Almendral MJ, Curto Y, Criado JJ, Rodriguez E, Manzano JL (2006) Determination of the DNA-binding characteristics of ethidium bromide, proflavine, and cisplatin by flow injection analysis: usefulness in studies on antitumor drugs. Anal Biochem 355:157–164
16. Liu G-D, Yang X, Chen Z-P, Shen G-L, Yu R-Q (2000) Interaction of metal complexes of bis (salicylidene)-ethylenediamine with DNA. Anal Sci 16:1255–1259
17. Routier S, Bernier J-L, Waring MJ, Colson P, Houssier C, Bailly C (1996) Synthesis of a functionalized Salen−Copper complex and its interaction with DNA. J Org Chem 61:2326–2331
18. Burrows CJ, Rokita SE (1994) Recognition of guanine structure in nucleic acids by nickel complexes. Acc Chem Res 27:295–301
19. Gravert DJ, Griffin JH (1996) In: Sigel A, Sigel H (eds) Metal ions in biological systems, vol 33. Marcel Dekker, New York, pp 515–536
20. Bhattacharya S, Mandal SS (1995) Ambient oxygen activating water soluble cobalt–salen complex for DNA cleavage. J Chem Soc Chem Commun 2489–2490
21. Cheng C-C, Jian Y-H, Lo C-J, Cheng J-W (1998) Design and characterization of a short HMG-1/DAT1 peptide that binds specifically to the minor groove of DNA. J Chin Chem Soc 45:619–624
22. Terenzi A, Barone G, Silvestri A, Giuliani AM, Ruggirello A, Liveri VT (2009) The interaction of native calf thymus DNA with Fe^{III}-dipyrido[3,2-a:2′,3′-c] phenazine. J Inorg Biochem 103:1–9
23. Routier S, Vezin H, Lamour E, Bernier J-L, Catteau J-P, Bailly C (1999) DNA cleavage by hydroxy-salicylidene-ethylendiamine-iron complexes. Nucl Acids Res 27:4160
24. Capolongo F, Giomini M, Giuliani AM, Matzanke BF, Russo U, Silvestri A, Trautwein AX, Barbieri R (1997) The interactions of Fe^{3+} ions with adriamycin studied by ^{57}Fe Mössbauer and electronic spectroscopies. J Inorg Biochem 65:115–122
25. Sigel A, Sigel H (eds) (1996) Interactions of metal ions with nucleotides, nucleic acids and their constituents, metal ions in biological systems, vol 32. Marcel Dekker, New York
26. Mohammed S, Ameerunisha B, Sounik S, Nethaji M, Chakravarty AR (2010) Iron(III) Schiff base complexes of arginine and lysine as netropsin mimics showing AT-selective DNA binding and photonuclease activity. J Inorg Biochem 104:477–484
27. Bottcher A, Grinstaff MW, Labinger JA, Gray HB (1996) Aerobic oxidation of hydrocarbons catalyzed by electronegative iron salen complexes. J Mol Catal A Chem 113:191–200

28. Liou YW, Wang CM (2000) Peroxidase mimicking: Fe(Salen)Cl modified electrodes, fundamental properties and applications for biosensing. J Electroanal Chem 481:102–109
29. Zimmer C, Wahnert U (1986) Nonintercalating DNA-binding ligands: specificity of the interaction and their use as tools in biophysical, biochemical and biological investigations of the genetic material. Prog Biophys Mol Biol 47:31–112
30. Bailly C, Chaires JB (1998) Sequence-specific DNA minor groove binders. Design and synthesis of netropsin and distamycin analogues. Bioconjug Chem 9:513–538
31. Goodsell DS, Kopka ML, Dickerson RE (1995) Refinement of netropsin bound to DNA: bias and feedback in electron density map interpretation. Biochemistry 34:4983–4993
32. Haikarainen A, Sipila J, Pietikainen P, Pajunen A, Mutikainen I (2001) Synthesis and characterization of bulky salen-type complexes of Co, Cu, Fe, Mn and Ni with amphiphilic solubility properties. J Chem Soc Dalton Trans 991–995
33. Bahramian B, Mirkhani V, Tangestaninejad S, Moghadam M (2006) Catalytic epoxidation of olefins and hydroxylation of alkanes with sodium periodate by water-soluble manganese (III)salen. J Mol Catal A 244:139–145
34. Matulis D, Rouzina I, Bloomfield VA (2000) Thermodynamics of DNA binding and condensation: isothermal titration calorimetry and electrostatic mechanism. J Mol Biol 296:1053–1063
35. Kumar CV, Asuncion EH (1993) DNA binding studies and site selective fluorescence sensitization of an anthryl probe. J Am Chem Soc 115:8547–8553
36. Silvestri A, Barone G, Ruisi G, Teresa M, Giudice L, Tumminello S (2004) The interaction of native DNA with iron(III)-N, N′-ethylene-bis(salicylideneiminato)-chloride. J Inorg Biochem 98:589–594
37. Dehkordi MN, Bordbar AK, Mehrgardi MA, Mirkhani V (2011) Spectrophotometric study on the binding of two water soluble schiff base complexes of Mn(III) with ct-DNA. J Fluoresc 21:1649–1658
38. Shahabadi N, Kashanian S, Darabi F (2010) DNA binding and DNA cleavage studies of a water soluble cobalt(II) complex containing dinitrogen Schiff base ligand: The effect of metal on the mode of binding. Eur J Med Chem 45:4239–4245
39. Rajendram A, Magesh CJ, Perumal PT (2008) DNA–DNA cross-linking mediated by bifunctional [SalenAl^{III}]$^{+}$ complex. Biochim Biophys Acta 1780:282–288
40. Mandal SS, Varshney U, Bhattacharya S (1997) Role of the central metal ion and ligand charge in the DNA binding and modification by metallosalen complexes. Bioconjug Chem 8:798–812
41. Hiort C, Lincoln P, Norden B (1993) DNA binding of DELTA and LAMBDA-[Ru(phen)2DPPZ]2^{+}. J Am Chem Soc 115:3448–3454
42. Revenga-Parra M, Garcia T, Lorenzo E, Pariente F (2007) Comprehensive study of interactions between DNA and new electroactive Schiff base ligands: application to the detection of singly mismatched Helicobacter pylori sequences. Biosens Bioelectron 22:2675–2681
43. Pyle AM, Rehmann JP, Meshoyrer R, Kumar CV, Turro NJ, Barton JK (1989) Mixed-ligand complexes of ruthenium(II): factors governing binding to DNA. J Am Chem Soc 111(8):3051–3058
44. Liu Y-J, Chao H, Tau L-F, Yuan Y-X, Wei W, Ji L-N (2005) Interaction of polypyridyl ruthenium(II) complex containing asymmetric ligand with DNA. J Inorg Biochem 99:530–537
45. Kelly JM, Tossi AB, Mc Conell DJ, OhUigin C (1985) A study of the interactions of some polypyridylruthenium(II) complexes with DNA using fluorescence spectroscopy, topoisomerisation and thermal denaturation. Nucl Acids Res 13:6017–6034
46. Neyhart GA, Grover N, Smith SR, Kalsbeck WA, Fairly TA, Cory M, Thorp HH (1993) Binding and kinetics studies of oxidation of DNA by oxoruthenium(IV). J Am Chem Soc 115:4423–4428
47. Meyer-Almes FJ, Porschke D (1993) Mechanism of intercalation into the DNA double helix by ethidium. Biochemistry 32:4246–4253
48. Fant K, Norden B, Lincoln P (2011) Using ethidium to probe nonequilibrium states of DNA condensed for gene delivery. Biochemistry 50:1125–1127
49. McGhee JD, Von Hipple PH (1974) Theoretical aspects of DNA-protein interactions: Co-operative and non-co-operative binding of large ligands to a one-dimensional homogeneous lattice. J Mol Biol 86:469–489
50. LePecq JB, Paoletti C (1967) A fluorescent complex between ethidium bromide and nucleic acids: physical–chemical characterization. J Mol Biol 27:87–106
51. Jennette KW, Lippard SJ, Vassiliades GA, Bauer WR (1974) Metallointercalation reagents 2-Hydroxy ethanethiolato (2,2′,2″-terpyridine)-platinum(II) monocation binds strongly to DNA by intercalation. Proc Natl Acad Sci U S A 71:3839–3843
52. Norden B, Tjerneld F (1982) Structure of methylene blue–DNA complexes studied by linear and circular dichroism spectroscopy. Biopolymers 21:1713–1734
53. Fang L, Kelley A, McMillin MR (1993) DNA-binding studies of Cu(bcp)2^{+} and Cu(dmp)2^{+}: DNA elongation without intercalation of Cu(bcp)2^{+}. J Am Chem Soc 115:6699–6704
54. OBrien R, Haq I (2004) Applications of biocalorimetry: binding, stability and enzyme kinetics. In: Ladbury JE, Doyle M (eds) Biocalorimetry. John Wiley and Sons Ltd, West Sussex
55. Chaires JB (1983) Equilibrium studies on the interaction of daunomycin with deoxypolynucleotides. Biochemistry 22:4204–4211
56. Breslauer KJ, Remeta DP, Chou WY, Ferrante R, Curry J, Zaunczkowski D, Snyder JG, Marky LA (1987) Enthalpy-entropy compensations in drug-DNA binding studies. Proc Natl Acad Sci U S A 84:8922–8926
57. Norden B, Kubista M, Kurucsev T (1992) Linear dichroism spectroscopy of nucleic acids. Q Rev Biophys 25:51–170
58. Norden B, Kurucsev T (1994) Analysing DNA complexes by circular and linear dichroism. J Mol Recognit 7:141–155
59. Sanchez-Cano C, Huxley M, Ducani C, Hamad AE, Browning MJ, Navarro-Ranninger C, Quiroga AG, Rodger A, Hannon MJ (2010) Conjugation of testosterone modifies the interaction of mono-functional cationic platinum(II) complexes with DNA, causing significant alterations to the DNA helix. Dalton Trans 39:11365–11374